Assessment of Tissue Damage due to Mechanical Stresses

Smita De[1], Paul Swanson[2], Mika Sinanan[3], Jacob Rosen[1], Aylon Dagan[1], and Blake Hannaford[1]

Biorobotics Laboratory, [1]Department of Bioengineering, [2]Department of Anatomic Pathology, [3]Department of Surgery
University of Washington
Box 352500, Seattle, WA 98195-2500
sd6@u.washington.edu

***Abstract* – While there are many benefits to minimally invasive surgery, force feedback, or touch sensation, is lacking in the currently available MIS tools, including surgical robots, creating the potential for excessive force application during surgery. The goal of this work was to develop a methodology with which to identify stress magnitudes and durations that can be safely applied with a grasper to different tissues, helping to improve MIS device design and reduce potential for clinically relevant consequences. Using the porcine model, stresses typically applied in MIS were applied to liver, ureter, and small bowel using a motorized endoscopic grasper. Acute indicators of tissue damage including cellular death, activation of the coagulation cascade, and infiltration of inflammatory cells were measured using histological and image analysis techniques. ANOVA and post-hoc analyses were used to detect stress magnitudes and durations that caused significantly increased tissue damage with the goal to ultimately identify safe stress 'thresholds' during grasping of the studied tissues. Preliminary data suggests a graded non-linear response between applied stress magnitude and apoptosis in liver and small bowel as well as granulocyte infiltration in small bowel.**

***Index Terms* – Tissue damage quantification, histology, minimally invasive surgery.**

I. Introduction

Minimally invasive surgery (MIS), both traditional and robot-assisted, provides a number of patient benefits including reduced incidence of infection, shorter hospital stays, and less pain [1, 2]. One current concern, however, is the lack of force feedback, or touch sensation, available to the surgeon for safe tissue manipulation, making it possible for a surgeon to cause tissue damage by inadvertently applying excessive stress to tissue [3, 4]. Surgical simulators, which can be used to help train surgeons in MIS techniques, usually do not include realistic portrayal of tissues during manipulation and many also lack force feedback [5]. Therefore, even during training, surgeons may not get a true sense of safe tissue handling.

A. Grasper induced damage

While there have been studies on complications and surgical stress due to surgical procedures at a macroscopic level, there is limited knowledge of localized short- and long-term effects of mechanical stresses on tissues due to surgical manipulations. Mechanical stress can cause unintentional injury to tissue by several means. One type of stress that might result in injury occurs during grasping for elevation, exposure, or manipulation purposes, maneuvers that can cause crushing of the tissue. By identifying stress magnitudes and durations within the range of those typically applied in MIS, that cause significantly increased injury, it may be possible to create a 'smart' surgical robot that can guide a surgeon to manipulate tissues with minimal resulting damage. In addition, surgical simulator design can be improved to reflect more realistic tissue responses and evaluate trainees' tissue handling skills.

B. Clinical Relevance

Stress injury from graspers may result in pathological scar tissue formation, bleeding, adhesions, and loss of bowel motility [6, 7]. Organs manipulated during MIS that may be injured in this way include liver, small bowel, and ureter. All three are susceptible to severe grasping injuries including perforation or hemorrhage [8, 9]. However, even less severe immediate injury can still result in clinically relevant consequences such as increased infection due to local breach of the bowel's protective barrier and adhesion formation [7, 10]. These effects may occur in a delayed fashion from interruption to the blood supply (ischemia), crushing of intracellular structures, or bursting of cells as well as from secondary consequences such as inflammation, coagulation, cellular death, and ischemia-reperfusion injury that may follow [11, 12, 13, 14].

C. Tissue Response to Injury

Three major aspects of tissue's acute response to injury include cellular changes, inflammation, and the consequences of vascular damage. The more severe cellular effects include apoptosis and necrosis, both forms

* This work is partially supported by the NSF (66-6531), the Army (62-8360), the Center for Videoendoscopic Surgery, and UW Department of Anatomic Pathology

of cell death. Inflammation includes infiltration of white blood cells (neutrophils, macrophages, and lymphocytes) and the respective chemical mediators that may be released. Vascular damage may include hemorrhage and activation of the coagulation cascade, which involves multiple steps, but ultimately results in the deposition of cross-linked fibrin [13]. Each of these three components of injury involve a large number of intermediate steps, including enzymatic activity, cellular responses, and chemical mediators that can reflect the injured state of a tissue.

D. Damage measurement

Little current data is available to suggest stress magnitudes and durations that are safe for tissue manipulation. Most previous studies have been qualitative in nature. For example, Elkins et al. evaluated the local injury to rabbit peritoneum from basic surgical maneuvers such as suturing, excising, and blunt abrasion. These injury sites were examined for acute markers of damage using histological staining, specifically hematoxylin and eosin or Masson-trichrome. White blood cell infiltrate, necrosis, fibrin deposition, and collagen formation were correlated with survival studies showing increased inflammation and necrosis associated with increased adhesion formation [15]. This observation suggests that acute markers of tissue injury could potentially predict long-term sequelae [14, 15, 16]. Studies specifically relating to tissue crush injury during grasping have also been qualitative. For example, Marucci et al. examined grasper trauma to the human gall bladder wall during laparoscopic cholecystectomies based on epithelial loss, interstitial hemorrhage, and focal thinning of the wall [9]. They found that increased grasp duration can lead to increased tissue damage.

Though not directly related to MIS, studies of a more quantitative nature have been done on the effects of handling tissues during open surgery. Thomas et al. have done multiple studies in rats quantifying cellular, subcellular, and biochemical changes to small bowel after manipulation, including cell viability and mitochondrial function [17, 18]. In another study, Klaff et al. quantified cellular infiltrates and changes in bowel muscularis function in rats from surgical manipulation. Their results indicated that gut paralysis is related to degree of trauma and the resulting inflammatory response [6]. Neither study quantified the severity of the compressions applied to the bowel.

E. Study design

In the present study, we sought to validate protocols to measure *in vivo* tissue damage as a function of the degree and duration of mechanical stress. The eventual goal of this work is to define stress levels that could be considered "safe" when applied to tissues in the course of routine MIS. As in the previous studies, many markers of coagulation, inflammation, and cell death can serve as localized indicators of injury. The relative abundance of such markers can be measured and used to assess the degree of tissue trauma. Our research group has previously recorded characteristics of surgeons' movements during animal MIS procedures. These included magnitudes and durations of applied forces and torques at the surgeon-MIS instrument interface [19]. For example, it was found that the mean grasp force applied was 8.52 ± 2.77 N and the mean 95% grasp time was 8.86 seconds. In the present study, we were able to utilize these data to apply stress magnitudes and durations that are typically applied during MIS.

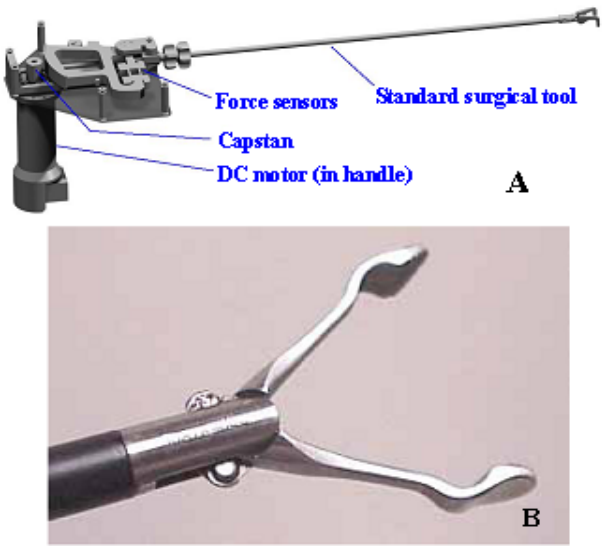

Figure 1. A) CAD drawing of the MEG. B) Close-up photograph of MEG's Babcock grasper end effector

II. METHODS

A. Grasping Device

The motorized endoscopic grasper (MEG) is a computer-controlled device developed for soft tissue testing [19]. Using the MEG, a series of calibrated compressive stresses was applied to tissues. The MEG is fitted with a Babcock type (flat, paddle-like atraumatic) surgical grasper. Fig. 1 shows a CAD drawing of the MEG and a photograph of the Babcock grasper end effector. The proximal end of the grasper tool is a ball joint that is connected to a partial pulley and cable. The motor in the MEG's handle is attached to a capstan and drives the cable and pulley mechanism. The rotation of the motor is converted to a linear translation of the grasper shaft at the ball joint, actuating the grasper jaws to open and close. Two strain gage force sensors (FR1010, 40 lb, Futek) are mounted in the pulley to measure applied forces on the pushrod. An encoder, also attached to the motor, records the position of the grasper jaws. Maximum force that can be applied by the MEG is 24.5N, which is well beyond the requirements of this study. The MEG was calibrated using springs with known spring constants. Current to the motor corresponding to a particular stress level can be calculated by the following equation [19] where grasper_area is 5.64×10^{-5} m^2:

Figure 2: *in vivo* image of liver with multiple compression sites (arrows). Lower stresses (60 kPa) begin at upper left with increasing stress magnitudes up to the highest stresses (240 kPa) at lower right.

$$i(Amp) = \sigma(N/m^2) \times \frac{grasper\_area(m^2)}{(40N/Amp)}. \quad (1)$$

Desired stresses were applied by controlling current applied to the motor. The actual applied forces were measured with the strain gage recordings. The measured forces and calculated stresses were used for data analysis.

B. Animal Experiment

This paper reports the results of a single animal experiment. The porcine model was chosen for this study because it is used for MIS training purposes and is commonly used as a model for human abdominal and pelvic organs [8]. On the day of experiment, an adult female farm pig (~30 kg) was placed under full IV and inhalation anesthesia by a veterinary technician. A laparotomy was performed to expose the organs. The MEG was used to apply compression stresses, between 0 and 300 kPa (typically 0, 60, 120, 180, 240 kPa), at regular intervals along the liver, small bowel jejunum, and ureter. 0 kPa served as the control. Compression stresses were held for 10 or 30 seconds. These parameters were based on previously collected data on surgical movements in MIS. Stresses that exceed tissue 'failure' were avoided. Each set of parameters was repeated at least three times (i.e. 60 kPa for 10 seconds on liver is repeated three times at three different sites). Fig. 2 shows liver after multiple stresses have been applied. The injury response was allowed to develop for three hours at which time animal was euthanized and the tissues were harvested and fixed for histology. The animal experiments were conducted in the Center for Videoendoscopic Surgery under an IRB approved animal use protocol (#2469-04).

C. Histology

Tissue processing and staining was done in the clinical and research histology laboratories in the Department of Pathology at the University of Washington. Tissues were fixed in 10% buffered formalin and embedded in paraffin. Standard 5 micron paraffin sections were mounted on glass. Sections were taken from each crushed tissue sample

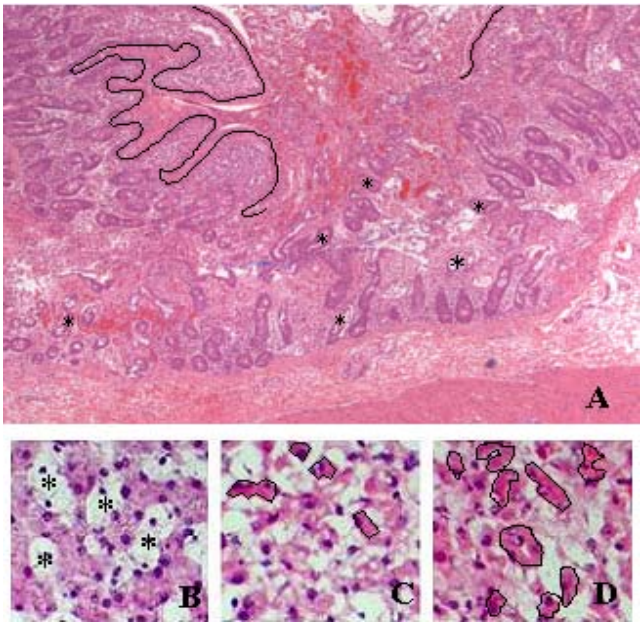

Figure 3: H&E stain A) Small bowel, 180 kPa, 40X. Clear destruction of villi, abnormal crypts (*), break in line indicates break in endothelial barrier. B-D) Liver, 400X. B) control (0 kPa), normal hepatocytes and sinusoids (*), (C) 100kPa , contracted cells and eosinophilia (outlined) with some normal hepatocytes, (D) 200kPa, increased eosinophilia (outlined), abnormal nuclei, and loss of sinusoids.

parallel to the direction of applied compressive stress. During initial examination, sections were stained with hematoxylin and eosin (H&E) for visualization of overall changes in morphology and architecture, as well as cellular death, which is marked either by increased cytoplasmic eosinophilia with nuclear pyknosis, or by overt apoptosis with nuclear fragmentation.

Fig. 3 shows examples of H&E stained tissues. Fig. 3A demonstrates injury to the small bowel mucosa with a clear breach of the small bowel protective barrier. Figs. 3B-D show changes in liver architecture and cellular morphology with increase in stress magnitude.

D. Inflammation

Granulocytes (neutrophils and eosinophils) were stained for myeloperoxidase (MPO) using polyclonal antibody (DakoCytomation) immunohistochemistry (IHC) [20]. All IHC analyses used a standard avidin-biotin-peroxidase complex (ABC) technique [21] following microwave-based epitope retrieval in 0.01 M citrate buffer (pH 6.0). 3,3'-diaminobenzidine 4HCl (DAB) was used as the

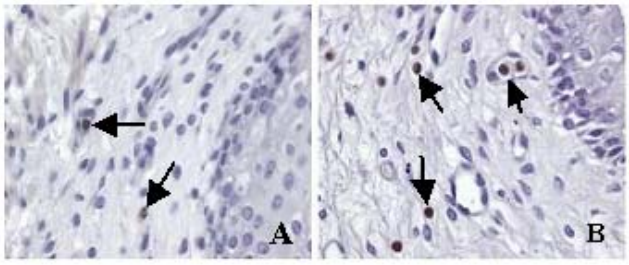

Figure 4: Ureter, 400X. Myeloperoxidase IHC for granulocytes (brown), A) control, B) 180 kPa. Arrows indicate granulocytes

chromogen and slides were counterstained with Harris hematoxylin. Fig. 4 shows ureter (control and 180kPa, 30 second grasps) with granulocytes demonstrating a cytoplasm-based anti-MPO reaction (granulocytes appear brown from the brown DAB precipitate (arrows)). Careful inspection of each labelled cell was required to separate granulocytes from other leukocytes, which may also be stained using this technique. Only stained cells with multi-lobed nuclei were counted as granulocytes. Because the blue/brown stain contrast in IHC preparations does not allow for evaluation of granule morphology, further separation of the granulocytes into neutrophils and eosinophils could be done based on nuclear properties.

E. Apoptosis

Activated caspase-3 antibody (polyclonal antibody, Cell Signaling Technologies) IHC was used to quantify apoptotic cell death with a methodology (including epitope retrieval) that was identical to that employed for myeloperoxidase [22]. Figs. 5A and 5B show apoptosis in small bowel (brown DAB precipitate in the cytoplasm and nuclear fragments of positive cells (arrows)) in control (0kPa) and injured tissue (285kPa), respectively.

F. Activation of Coagulation Cascade

Initial examination of activation of the coagulation cascade was based on observed areas of clot formation in H&E stained sections.

G. Quantification and Image Analysis

Multiple images within the crush site were taken from several sections of each injury site at 400X. The images were taken from the center of the crush injury site. Based on engineering principles, the center region is most representative of the average measured stress. Granulocytes were manually counted within a field of view. Measurement of apoptotic cells was done using ImageJ, image analysis software available through the NIH website (http://rsb.info.nih.gov/ij/). Image analysis was used to determine percent area of apoptotic cells in a field of view because apoptotic cells ultimately fragment and cannot be counted. Quantification was based on the total number of pixels (i.e. area) within a field of view that was marked by the respective antibody. The background was subtracted from the original image and then split into its RGB components. A manually identified threshold was applied to the blue channel and the percent area of staining was determined. Figure 5 shows results of IHC and image analysis for identifying and quantifying labelled cells within the crush area. Figure 5A (0 applied stress) illustrates normal cell turnover (apoptotic cells are brown). Figure 5B is of crushed small bowel (285kPa) with an increase in apoptotic cells. Figures 5C and 5D show the blue channel of Figures 5A and 5B, respectively, after background removal and RGB split. Figures 5E and 5F show the final post-threshold images of 5A and 5B, respectively, where black represents the apoptotic cells originally stained brown. Between 9 - 12 images were collected from at least 3 different crush sites in one animal for each set of stress parameters analysed and reported here.

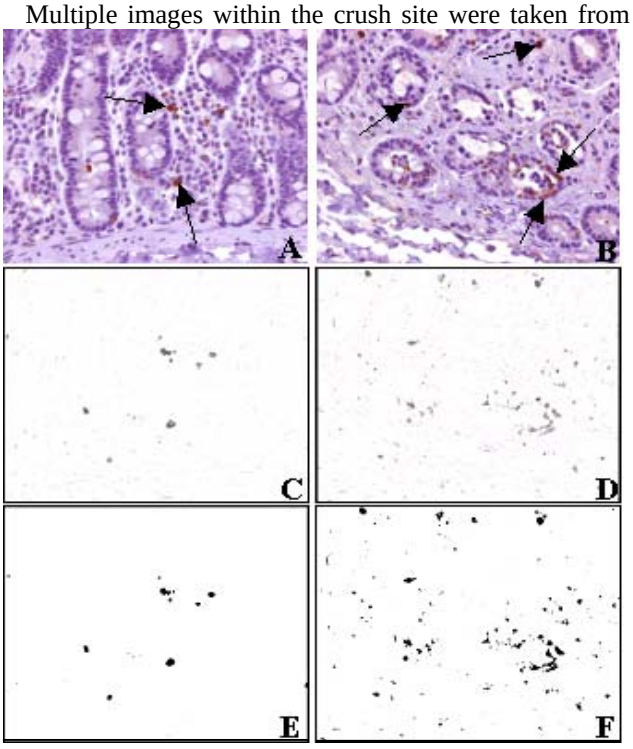

Figure 5: Small bowel, 400X. A & B) Control and 285kPa, respectively. Caspase-3 IHC, original images, arrows indicate apoptotic cells. C & D) Blue channels of A & B after background subtraction and RGB split. E & F) Final post-threshold images of A & B.

H. Statistics

The Matlab statistics toolbox and Microsoft Excel were used for statistical analyses. ANOVA analyses were completed for each organ and tissue damage parameter pair (i.e. liver, apoptosis) with the independent variable being stress magnitude or duration. Multiple comparison tests were done if there was evidence of significant differences. A p-value equal to or less than 0.05 was considered significant.

III. Preliminary Results

Stress application with the MEG was repeatable with low variance. Horizontal error bars indicate standard deviation of applied stress, which was less than 6% of applied stress magnitude for all conditions (Figs. 6, 7, and 8).

A. Granulocytes

The number of granulocytes increased with stress magnitude in small bowel after 30 second grasps (Figure 6). Statistical analyses indicate a significant difference between the control group and both the 180 kPa and 240 kPa groups.

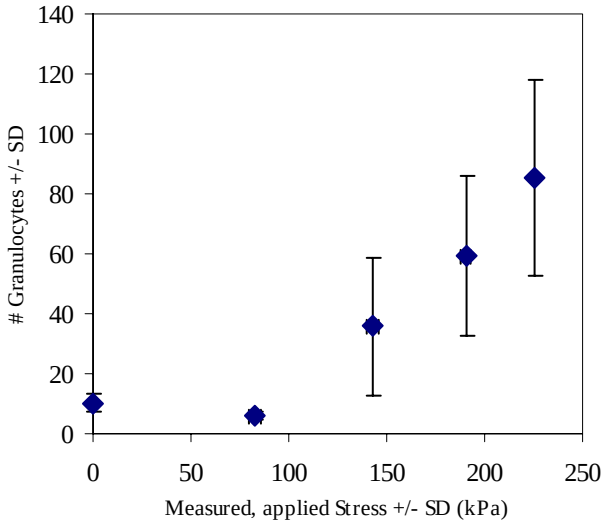

Figure 6: Small Bowel, 30 second grasp. Number of granulocytes versus applied stress magnitude.

B. Apoptosis

In liver subjected to 30 second grasps, percent apoptotic labelled pixels increased with stress magnitude (Figure 7). ANOVA analyses followed by multiple comparison tests indicated that there was significantly increased apoptosis with 180kPa and 240kPa compared to each other and the control.

Again, percent apoptotic labelled pixels increased with stress magnitude for both 10 and 30 second grasps in small bowel (Figure 8). There was no significant difference between the responses with respect to grasp duration. For the 10 second grasp, 240 kPa resulted in significantly greater apoptosis compared to all other stress groups. There was also a significant difference between 240 kPa and the control with a 30 second grasp.

An increase in apoptosis with increasing stress magnitude was observed in ureter, but the difference between the stress groups was not significant based on ANOVA analysis.

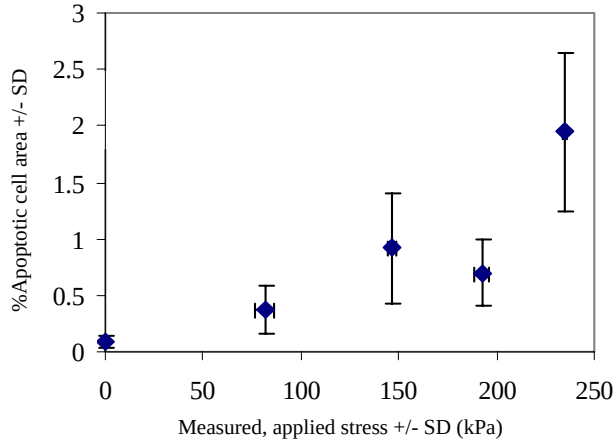

Figure 7: Liver, 30 second grasp. Apoptotic labelled cell area versus applied stress magnitude.

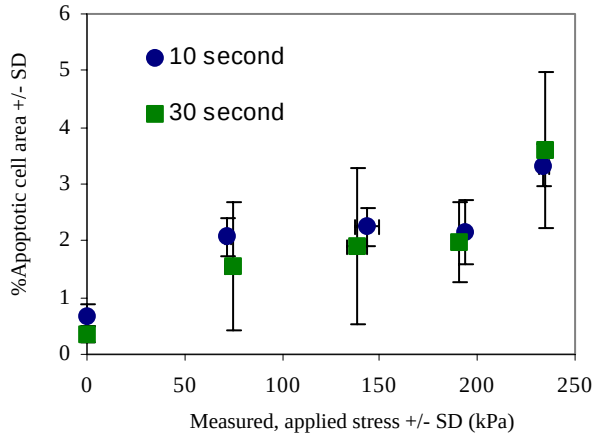

Figure 8: Small bowel, 10 and 30 second grasps. Apoptotic labelled cell area versus applied stress.

C. Coagulation

Visual examination of H&E stained sections of small bowel and liver showed increased areas of clot formation with increasing stress magnitude. No obvious difference was observed in ureter.

IV. Discussion

Identification of stress magnitudes and durations that cause minimal trauma to patient organs during manipulation may help alleviate pain and avoid potentially significant consequences in MIS by helping guide a surgeon safely manipulate tissues. In addition, surgical simulators may be improved to have more realistic tissue responses as well as feedback regarding trainees' handling of tissues. In order to identify such stress 'thresholds' and stress dose responses, we must first determine an appropriate methodology that will include quantitative techniques for both the stresses applied and the resultant tissue damage. We used a device that was specifically designed for soft tissue testing, to apply known stresses to tissues, providing us with the quantitative independent variables of stress duration and magnitude. Based on our preliminary results, the MEG is an appropriate tool for our purposes. Desired stresses were applied and measured with minimal standard deviations within each group.

To assess the tissue damage resulting from compression stresses, we used histology for measuring three major aspects of tissue's response to injury: cell death, inflammation, and activation of the coagulation cascade. Our preliminary data showed a dose-dependent response to stress magnitude as indicated by apoptosis in all three tissues as well as granulocytes in small bowel. ANOVA analyses indicated statistically significant differences in tissue damage between stress magnitudes in multiple tissues and with multiple measures of injury. This result within one animal suggests that the histological methods selected are sensitive enough to distinguish between varying levels of injury within our range of interest in liver and small bowel. Statistically significant differences were

not seen with resulting damage in ureter; however, this may be representative of this tissue's response rather than the sensitivity of our assays.

The last step in finalizing our methodology will involve analysis of the remaining sets of stress parameters. We will include an additional stress duration of 60 seconds as suggested by the aforementioned Blue Dragon results. We will also include a quantitative measure for fibrin to represent activation of the coagulation cascade. This will be done using IHC analyses with a monoclonal anti-fibrin antibody (1H10; from Dr. Gaffney, Department of Surgery, St. Thomas Hospital, London), using the detection and image analysis methods described above. Immunoreactivity commensurate with fibrin deposition can be used as a marker of activation of the coagulation cascade [23].

Based on these preliminary results and the expected results from the remaining analyses, we believe this methodology is valid for our goals. Thus, we will begin using these techniques to begin identifying damage 'thresholds' and stress dose response curves for multiple organs.

ACKNOWLEDGMENTS

We would like to thank the Center for Videoendoscopic Surgery and the Department of Anatomic Pathology at the University of Washington for the use of space, supplies, and expertise. We would also like to acknowledge Dr. Gaffney, Department of Surgery, St. Thomas Hospital, London for the use of the fibrin antibody and members of the UW Biorobotics laboratory for their support.

REFERENCES

[1] P. Yuen, et al., "Metabolic and Inflammatory Responses after Laparoscopic and Abdominal Hysterectomy," *Am. J. Obstet. Gynecol*., vol 179, pp. 1-5, 1998.

[2] H. Miyake, et al, "Comparison of Surgical Stress between Laparoscopy and Open Surgery in the Field of Urology by Measurement of Humoral Mediators," *Int. J. Urol.*, vol 9, pp. 329-33, 2002.

[3] B. Bethea, et al., "Application of Haptic Feedback to Robotic Surgery," *J. Laparoendosc. Adv. Surg. Tech. A*, vol 14, pp. 191-5, 2004.

[4] J. Bodner, H. Wykypiel, G. Wetscher, and T. Schmid, "First Experiences with the da Vinci Operating Robot in Thoracic Surgery," *Eur. J. Cardiothorac. Surg.*, vol 25, pp. 844-51, 2004

[5] L. Thurfjell, A. Lundin, and J. McLaughlin, "A Medical Platform for Simulation of Surgical Procedures," *Stud. Health Technol. Inform*., vol 81, pp. 509-14, 2001.

[6] J. Kalff, W. Schraut, R. Simmons, and A. Bauer, "Surgical Manipulation of the Gut Elicits an Intestinal Muscularis Inflammatory Response Resulting in Postsurgical Ileus," *Ann. Surg.*, vol 228, pp. 652-63, November 1998.

[7] R. Anup and K. Balasubramanian, "Surgical Stress and the Gastrointestinal Tract," *J. Surg. Res.*, vol 92, pp. 291-300, August 2000. Review.

[8] E. Heijnsdijk, J. Dankelman, and D. Gouma, "Effectiveness of Grasping and Duration of Clamping using Laparoscopic Graspers," *Surg. Endosc*., vol 16, pp. 1329-31, 2002.

[9] D. Marucci, et al., "Grasper Trauma during Laparoscopic Cholecystectomy," *Aust. N. Z. J. Surg*., vol 70, 5788-1, 2000.

[10] P. Reissman, T. Teoh, K. Skinner, J. Burns, and S. Wexner, "Adhesion Formation after Laparoscopic Anterior Resection in a Porcine Model: a Pilot Study," *Surg. Laparosc. Endosc*., vol 6, pp. 136-9, April 1996.

[11] H. Ceylan, et al., "Temporary Stretch of the Testicular Pedicle may Damage the Vas Deferens and the Testis," *J. Pediatr. Surg*., vol 38, pp. 1530-3, 2003.

[12] R. Shi and J. Pryor, "Pathological Changes of Isolated Spinal Cord Axons in Response to Mechanical Stretch," *Neuroscience*, vol 110, pp. 765-777, 2002.

[13] R. Cotran, V. Kumar, and T. Collins, Pathological Basis of Disease, 6th ed. Pennsylvania: Saunders, 1999.

[14] A. Donati, et al., "Predictive Value of Interleukin 6 (IL-6), Interleukin 8 (IL-8) and Gastric Intramucosal pH (pH-i) in Major Abdominal Surgery," *Intensive Care Med.* vol 24, pp. 329-35, 1998.

[15] T. Elkins, T. Stovall, J. Warren, F. Ling, and N. Meyer, "A histologic evaluation of peritoneal injury and repair: Implications for adhesion formation," *Obstet. Gynecol*., vol 70, pp. 225-228, 1987.

[16] A. Ar'Rajab, et al., "The Role of Neutrophils in Peritoneal Adhesion Formation," *J. Surg. Res*., vol 61, pp. 143-6, 1996.

[17] T. Simmy, R. Prabhu, and K. Balasubramanian, "Surgical Manipulation of the Intestine and Distant Organ Damage-Protection by Oral Glutamine Supplementation," *Surgery*., vol 137, pp. 48-55, January 2005.

[18] T. Simmy, R. Anup, R. Prabhu, and K. Balasubramanian, "Effect of Surgical Manipulation of the Rat Intestine on Enterocyte Populations," *Surgery*, vol 130m, pp. 479-88, September 2001.

[19] J. Brown, In-Vivo and Postmortem Biomechanics of Abdominal Organs Under Compressive Loads: Experimental Approach in a Laparoscopic Surgery Setup, University of Washington, thesis, 2003.

[20] G. Pinkus and J. Pinkus, "Myeloperoxidase: a Specific Marker for Myleoid Cells in Paraffin Sections," *Mod. Pathol.*, vol 4, pp. 733, 1991.

[21] S. Hsu, K. Yang, and E. Jaffe, "Phenotypic Expression of Hodgkin's and Reed-Sternberg Cells in Hodgkin's Disease," *Am. J. Pathol*., vol 118, pp. 209-17, 1985.

[22]A. Gown and M. Willingham, "Improved Detection of Apoptotic Cells in Archival Paraffin Sections: Immunohistochemistry using Antibodies to Cleaved Caspase 3," *J. Histochem. Cytochem.*, vol 50, pp. 449-54, 2002.

[23]T. Edgell, F. McEvoy, P. Webbon, and P. Gaffney, "Monoclonal Antibodies to Human Fibrin: Interaction with other animal fibrins," *Thromb. Hemo.*, vol 75, pp. 595-9, 1996.